Sensors & Actuators: B. Chemical 422 (2025) 136652

Contents lists available at ScienceDirect

Sensors and Actuators: B. Chemical

journal homepage: www.elsevier.com/locate/snb

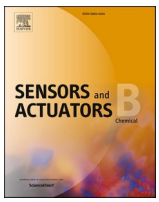

High-precision micro-total analysis of sodium ions in breast milk

Huilu Bao [a], Xiao Fan [a], Xiaoyu Zhang [a], Xin Zhang [a], Katie T. Kivlighan [b], Sallie S. Schneider [c], Jianghong Liu [d], Alan T. Charlie Johnson [e], Kathleen F. Arcaro [f], Jinglei Ping [a,g,*]

[a] Department of Mechanical and Industrial Engineering, University of Massachusetts Amherst, Amherst, MA 01003, USA
[b] College of Nursing, University of New Mexico, Albuquerque, NM 87131, USA
[c] Pioneer Valley Life Sciences Institute, Springfield, MA 01199, USA
[d] School of Nursing, University of Pennsylvania, Philadelphia, PA 19104, USA
[e] Department of Physics and Astronomy, University of Pennsylvania, Philadelphia, PA 19104, USA
[f] Department of Veterinary and Animal Sciences, University of Massachusetts, Amherst, MA 01003, USA
[g] Institute for Applied Life Sciences, University of Massachusetts Amherst, Amherst, MA 01003, USA

ARTICLE INFO

Keywords:
Lab on a chip
MicroTAS
Breast milk
Sodium ions
Micro electrodialysis
Ion-selective field-effect transistor
Graphene

ABSTRACT

Measuring sodium ion concentration in breast milk can provide crucial health information for both mother and infant, including early signs of low-grade infection and reduced milk supply. Traditional sensing methods are slow, bulky, expensive, and require skilled operators. Here, we develop a coverslip-sized, high-precision lab-on-a-chip device that processes and detects sodium ions in human breast milk. The device uses micro-electrodialysis to extract sodium ions into a simple acceptor solution with 92 ± 3 % efficiency and employs a graphene ion-selective sensor for high-performance quantification. We demonstrate a straightforward calibration strategy, enabling the device to measure breast-milk sodium ion levels in 141 seconds, with accuracy comparable to inductively coupled plasma mass spectrometry. Our approach offers a promising pathway to efficient, point-of-care diagnosis of conditions associated with metal-ion levels in complex liquid-biopsy samples.

1. Introduction

Monitoring sodium levels in breast milk holds significant potential for averting premature cessation of breastfeeding and safeguarding the health of both mother and infant. Health organizations recommend exclusive breastfeeding for the first 6 months of a new-born's life [1,2], yet only 25 % of mothers in the United States meet this guideline [1], largely due to concerns about insufficient milk supply and consequent failure to meet personal lactation goals [3]. A growing body of literature identifies subclinical mastitis (SCM), an asymptomatic inflammatory condition that leads to increases in the permeability of the mammary gland epithelial cell layer through impacting the sodium-potassium (Na/K) balance in breast milk and the milk supply [4], as a contributing factor to the shortage of milk supply [5]. As a result, the sodium-ion concentration ($[Na^+]$) in breast milk serves as a crucial biomarker for diagnosing SCM. Additionally, breast-milk $[Na^+]$ is also highly indicative of secretory activation (the time point when the mammary epithelial cells first secrete copious milk) [6].

Inductively coupled plasma mass spectrometry (ICP-MS) is the gold-standard method to determine breast milk $[Na^+]$ [7,8]. However, its practical application in affordable medical or point-of-care scenarios is limited due to its complex pre-processing requirements, large size, and high cost [9]. Alternatively, compact benchtop devices based on polymeric membrane-based ion-selective electrodes (ISE) [10] are widely used for quantifying $[Na^+]$ in various biofluids [11,12]. Yet, their detection limit is unsatisfactory, with the lowest level being only 20 mM (typically, breast-milk $[Na^+]$ ranges between 3 and 20 mM). Furthermore, factors such as rigidity and need for regular solution replenishment — owing to the configuration of a reference electrode immersed in a solution reservoir — limit their ease of use [13]. Consequently, a convenient, cost-effective, and miniaturized device for detecting $[Na^+]$ in breast milk remains an urgent, unmet need.

We develop a coverslip-sized total analysis device that automates necessary steps for high-precision chemical analysis of sodium ions in minimally processed breast milk. As shown in Fig. 1, the device consists of a microelectrodialysis (μED) processor for extracting sodium ions and a sodium sensor based on a graphene ion-sensitive field effect transistor (G-ISFET). Our result demonstrates that, when they work together in the total analysis device, the output solution from the μED processor is sufficiently simplified for precise analysis by the G-ISFET Na^+ sensor,

* Corresponding author at: Department of Mechanical and Industrial Engineering, University of Massachusetts Amherst, Amherst, MA 01003, USA.
E-mail address: ping@engin.umass.edu (J. Ping).

https://doi.org/10.1016/j.snb.2024.136652
Received 22 July 2024; Received in revised form 10 September 2024; Accepted 17 September 2024
Available online 17 September 2024

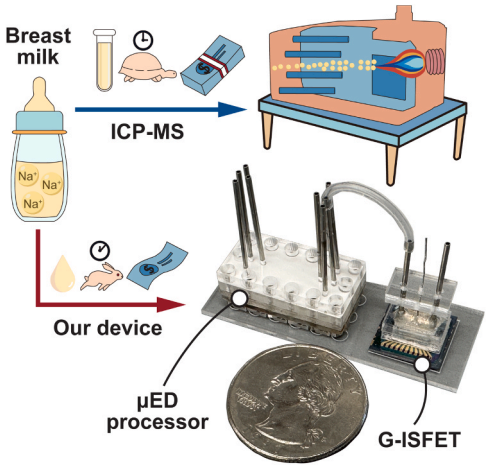

Fig. 1. Breast-milk sodium analytical techniques. Compared to ICP-MS, our coverslip-sized device outperforms in size, sample consumption, time, cost, and ease of use, without compromising detection accuracy.

with readout accuracy comparable to that of ICP-MS, while its efficiencies in time (3 min vs 30 min), cost per tool (approximately $20 vs $180000), cost per test ($1 vs $110), and sample consumption (10–20 μL vs mL) are all enhanced by orders of magnitude. (See Table 1 for comparison in metrics between our method and other methods.)

2. Material and methods

2.1. Microelectrodialysis processor

The μED processor is fabricated using scalable material-preparation and device-manufacturing methods (See Methods in Supporting Information). As shown in Fig. 2a, four fluidic channels, each with a length of 10 mm, are laser-cut on acrylic plates measuring 25 × 13 × 0.2 mm. The acrylic plates with two anion exchange membranes (AEMs) and a cellulose dialysis membrane are assembled using adhesive polypropylene films. The assembly is sandwiched between two acrylic chassis with two platinum-sheet electrodes integrated into the structure. On the top of the μED processor, eight fluid inlets and outlets are connected to stainless-steel tubes (Fig. 1). The μED processor is ~100× miniaturized in volumetric dimension compared to previous devices of the same type [14].

As shown in Fig. 2b and c, the four channels of the μED processor from top to bottom are: the isolator channel, the sample channel, the acceptor channel, and the second isolator channel. In this order, these channels let flow deionized (DI) water, sample solution, 50 mM HNO_3 solution, and 300 mM HNO_3-acidified 2-(N-morpholino) ethanesulfonic acid (MES) buffer at a pH of 2.1, at flow rates of 1500 μL min^{-1}, 25 μL min^{-1}, 25 μL min^{-1}, and 1500 μL min^{-1}, respectively, controlled by a set of valves and syringe pumps [14–16]. The 25 μL min^{-1} sample flow rate allows that each sample section spends 17 seconds passing through the fluid channel. Each extraction process takes 41 seconds, after which the volume of the acceptor solution released at the corresponding channel's outlet is 17 μL, matching the volume of the Na^+ sensor's fluidic channel.

In the μED extraction process, a current bias is applied between the platinum-sheet electrodes, to drive cations, including the target sodium ions, toward the cathode through the dialysis membrane and into the acceptor solution. The cations are collected and concentrated in the acceptor solution, while impurities in breast milk with dimensions larger than the dialysis membrane's pore size (1.32–1.42 nm), including lipids, proteins, enzymes, and microorganisms [17], remain in the sample solution. The use of AEMs maximizes ion extraction efficiency and reliability: the AEM near the anode prevents proton transfer, thereby inhibiting pH variation in the acceptor solution; the AEM near the cathode prevents the transfer of sodium ions into the isolator solution. The solution from the outlet of the acceptor channel is either collected for quantification by ICP-MS or directed to the G-ISFET sensor on the same device for sodium detection.

Table 1
Comparison of metrics among different breast-milk sodium-ion detection methods.

	Our method	ICP-MS	ISE
Detection time	< 3 min	~ 30 min [32]	< 3 min [33]
Size	Coverslip -sized	Full-sized benchtop	Compact benchtop
Cost/tool	~ $ 20	~ $ 180,000 [34]	~ $ 3500 [35]
Cost/test	~ $ 1	~ $ 110[36]	~ $ 1 [37]
Sample consumption	10–20 μL	mL [32]	60–400 μL [33]
Ease of use	High	Low	Low
Is detection limit favorable?	Yes	Yes	No

2.2. Sodium ion sensor

The G-ISFET Na^+ sensor, as shown in Fig. 3a, consists of a microfluidic chip, a Na^+-selective membrane based on sodium ionophore [18], an array of graphene field-effect transistors (G-FETs; Fig. 3b), and a Pt-wire liquid gate. The graphene used for fabricating ISFET channels is a monolayer synthesized through low-pressure chemical vapor deposition (LPCVD) on a copper-foil substrate (see Methods in Supporting Information). The ionophore membrane, which is 40-μm thick and selective to sodium ions, is fabricated on the graphene channel of the G-FET, forming a G-ISFET Na^+ sensor. The membrane is highly selective to Na^+, with a permeability 20 times greater than that for other metal ions [19], minimizing the non-specific response of the sensor and potential biofouling to the graphene channels [20]. Additionally, G-ISFETs show a lifespan of up to 6 months [21] and demonstrate high stability (25 nA/h drift) [22]. When the solution containing analyte sodium ions is loaded into the microfluidic channel over the graphene channel, sodium ions from the solution diffuse through the membrane, reach the graphene channels, and establish isothermal absorption equilibrium, as shown in Fig. 3c. A Pt wire is used as a liquid gate and the drain-to-source current of the G-ISFET is measured. The sensor is integrated with the sample processor in a microfluidic device, making it the first of its kind [19–21] and uniquely suitable for development in point-of-use applications.

2.3. Breast-milk sodium detection

Before testing breast-milk samples, the G-ISFET Na^+ sensor is calibrated by measuring the current response to three standard NaCl solutions at low concentrations of 0.25 mM, 0.5 mM, and 0.75 mM, respectively. The data are fitted using a proportional function, where the slope represents the sensitivity of the response-concentration relationship. The calibration curve is obtained by extrapolating this linearly fitted curve.

The breast milk samples are pretreated by a centrifuge and loaded into the μED processor. The outputting acceptor solution from the processor is loaded into the G-ISFET Na^+ sensor. Using the calibration curve, the measured G-ISFET current is converted to sodium-ion concentration. Sodium-ion concentrations in the breast-milk samples are also measured by using ICP-MS and ISE analyses.

3. Results and discussion

3.1. Microdialysis

Fig. 4 shows the transfer efficiency of the μED processor for Na^+-extraction, which is defined as the ratio of [Na^+] in the acceptor solution

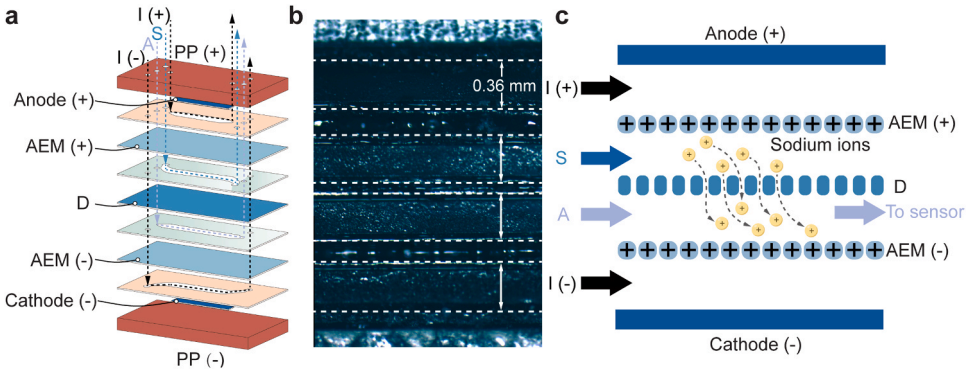

Fig. 2. The μED processor and the G-ISFET Na^+ sensor. a Explosion view of the μED processor with two polymethyl methacry-late (PMMA) plates, PP (+) and PP (-), each contains a cassette to host the anode/cathode. I (+) and I (-) represent the isolator channels. AEM (+) and AEM (-) are the anion exchange membranes. S stands for the sample solution channel and A the acceptor channel. D is the dialysis membrane. b Optical microscopic image of the cross-section of the μED processor. The dashed white lines represent the boundaries of the fluidic channels. The widths of the channels, indicated by the double arrows, are identical. c Schematic diagram of the processor for the microelectrodialysis of breast milk. The curved dash arrows show the migration of the target sodium ions.

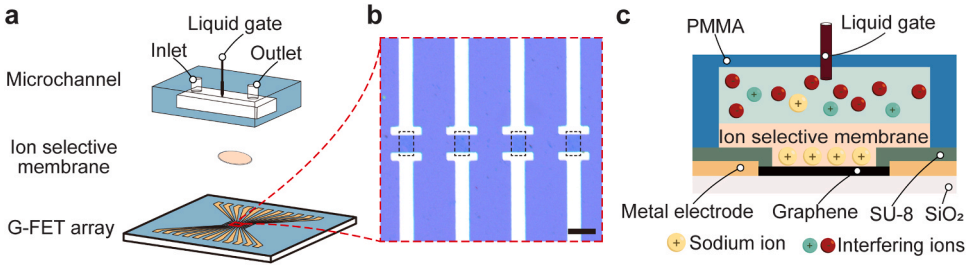

Fig. 3. The G-ISFET Na^+ sensor. a Explosion view of the Na^+ sensor. b Optical microscopic image of the G-FET array prior to applying the SU-8 passivation layer. The graphene channels are enclosed by the dashed black boxes. The scale bar is 100 μm. c Schematic diagram of the working principle of the G-ISFET for detecting Na^+ concentrations.

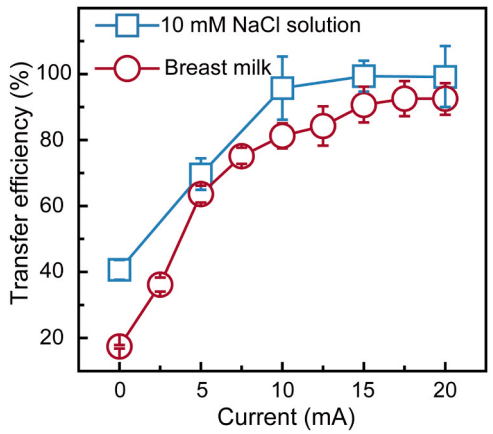

Fig. 4. Na^+ transfer efficiency as a function of the applied current across the electrolytic electrodes in the μED processor. The error bars represent standard deviations from multiple measurements.

after μED processing to that in all solutions after μED processing [23,24]. The transfer efficiencies achieved are 99 % for the NaCl solution and 92 % for breast milk, with an optimal driving electric current of 17.5 mA. The μED process is highly reliable: in various breast-milk extraction experiments using different devices, the standard deviation of the maximal extraction efficiencies is only 3 %.

3.2. Detection of sodium ions in buffer solutions

The G-ISFET Na^+ sensors are used to measure the sodium ion concentrations of NaCl solutions. As shown in Fig. 5a, after a 300-second incubation period following solution delivery, there is a leftward shift in the I-V_g characteristics of the graphene, due to variation in the charge carrier density of the graphene through the chemical gating effect [25,26]. Therefore, within the hole domain of the I-V_g curves [21], the source and drain current decreases as [Na^+] increases. Fig. 5b shows that the changes in the current (under a gate voltage of 0.4 V) linearly correlated with [Na^+] in NaCl solutions, with a constant sensitivity (the slope of the linear current-concentration relationship).

We also perform real-time measurement using NaCl solutions. As shown in Fig. 5c and inset, the current stabilizes within 15–100 seconds after the loading of solution, consistent with the Na^+ diffusion time [27] for the tested range of sodium-ion concentrations and comparable to previous results obtained using G-ISFETs with similar sodium ion selective membranes [19,28]. This short diffusion time represents the detection time of our method and reflects its high time efficiency. The relationship between current and sodium ion concentration is linear, indicating a well-defined sensitivity. The detection limit, determined by calculating the ratio of the standard deviation of current measurements to the sensitivity, is 10 μM, low enough for accurate quantification of [Na^+] at the lower end of this range (3 mM), owing to the high carrier mobility [29] and high chemical stability [30] of graphene [22,31]. The detection limit and the linear response-concentration relationship are further confirmed by real-time measurement over a broader range of [Na^+], as shown in Fig. S1 in the Supporting Information.

In our measurement, deviations in stabilized current range between 9 nA and 90 nA. Given the sensor's sensitivity (from -0.72 μA mM^{-1} to -3.05 μA mM^{-1}), these deviations minimally affect overall precision, with an impact of < 0.12 mM.

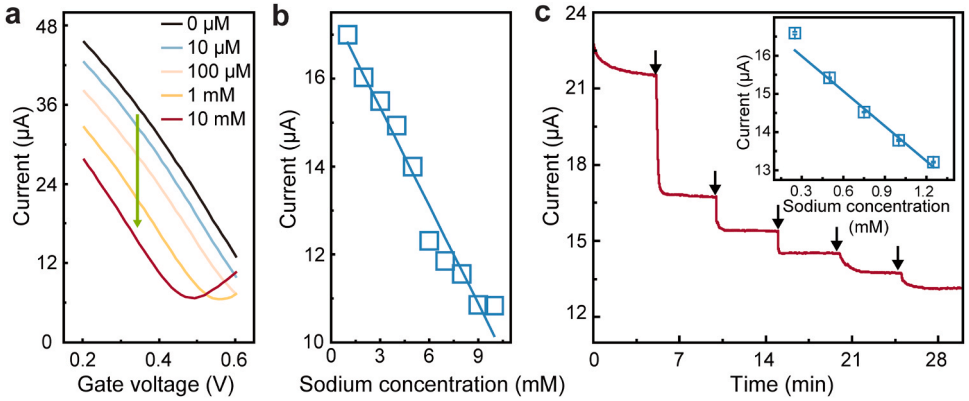

Fig. 5. The G-ISFET Na^+ sensor in response to standard NaCl solutions. a Typical I–V_g curves at varying [Na^+]. The arrow indicates a decrease in current as [Na^+] increases. b Transistor current versus [Na^+], at a liquid gate voltage of 0.4 V, using the same device as that on which device a is based. The error bars, determined from current readout uncertainties, are much smaller than the data points. The solid line represents a linear fit to the data. The sensitivity (the slope of the linear fit) is -0.74 μA mM^{-1}. c Real-time measurement of the current, using a different device from the one on which a and b are based. The arrows indicate the time points at which NaCl solutions of varying [Na^+] are loaded into the device. The inset shows the relationship between the stabilized current and the corresponding concentration. The error bars represent the uncertainties in the stabilized current readouts. The sensitivity is -3.05 μA mM^{-1}.

3.3. Detection of sodium ions in breast milk

Calibration is crucial before it is used with breast milk samples, due to the variability in the sensor sensitivity — which depends on the graphene's mobility and doping level and can differ from one device to another — and other sensor response variabilities caused by potential factors such as the thickness and permeability of the sodium-selective membrane and other manufacturing-induced device-to-device variations. Our calibration method leverages the linearity of the current-[Na^+] relationship and employs three standard NaCl solutions: 0.25 mM, 0.50 mM, and 0.75 mM, all well below the lowest Na^+ concentration found in human breast milk (~2 mM). This approach offers two advantages: (1) it requires a minimal number of data points needed to establish a linear relationship with satisfactory uncertainty, and (2) it minimizes the impact of potential Na^+ residue from the calibration procedure on detection accuracy. Fig. 6a shows the calibration curve of a G-ISFET Na^+ sensor, and measurement results of [Na^+] in breast-milk samples from five individuals using this curve. The quantified [Na^+] values well align with the calibration curve, indicating the effectiveness of the calibration method and the high selectivity of the ion-selective membrane. The entire process with our device, from loading a sample into the μED processor to receiving the sensor's readout, takes 141 seconds per sample, representing the end-to-end detection time of our method (Table 1).

Fig. 6b shows the breast-milk sodium-ion concentrations quantified by our device, compared with measurements from ICP-MS and compact benchtop ISE. The results from our device closely match those from the ICP-MS benchmark, with concentration disparities ranging from 0.04 mM to 0.39 mM and percent deviations from 1.3 % to 9.3 %. The maximal disparity observed (0.39 mM) is significantly lower, by more than an order of magnitude, than the minimum sodium-ion concentration found in human breast milk (~2 mM), reflecting the high resolution of the device.

In contrast, the ISE tool, while comparable in speed and cost/test to our device (Table 1), shows significantly lower accuracy, with absolute deviations from the ICP-MS benchmarks ranging from 2.42 mM to 4.27 mM, values comparable to the sodium-ion concentrations in human breast milk. The percentage deviations between ISE results and the benchmark ICP-MS results range from 51.8 % to 221.3 %. The overall ISE readings were higher than the actual concentrations since the ISE tool does not provide reliable results for sodium concentrations below 20 mM while the sodium ion concentrations in the breast milk samples were less than 7 mM. The advantage in accuracy of our method compared to ISE is demonstrated in the Bland-Altman plot (Supporting

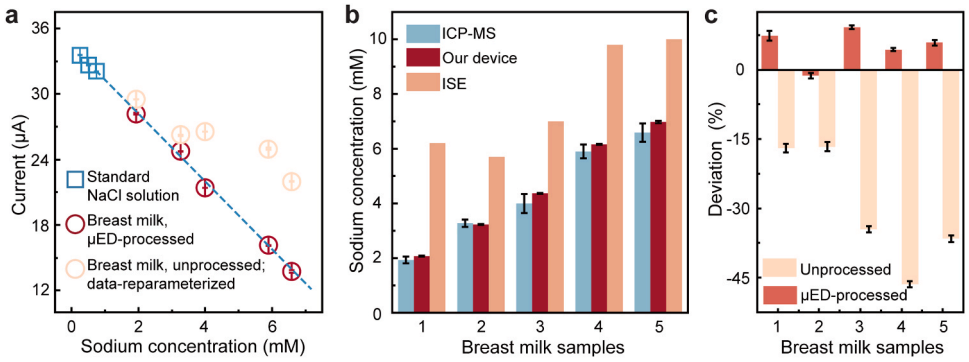

Fig. 6. Performance of our end-to-end device for total analysis of breast-milk [Na^+]. a The electric current measured by our devices, with breast-milk samples whether μED processed or not, versus the actual sodium-ion concentration quantified by ICP-MS. The unprocessed data are reparameterized by the ratio of the sensitivity of the device that tests μED-processed samples to that of the device that tests unprocessed samples. The dashed line is based on the linear fit for the μED-processed data from the standard NaCl solutions. The sensitivity (the slope of the linear fit) is -2.94 μA mM^{-1}. b Comparison of quantified [Na^+] using three different methods. c Deviations in quantified Na^+ concentrations between the G-ISFET Na^+ sensor and ICP-MS, for samples undergoing μED compared to those that do not. For the data obtained from our device, in a (y-axis), b and c, the error bars are based on the standard deviations of real-time current measurements. For the data based on ICP-MS in b, the error bars represent the standard deviation of multiple measurements. Error bars for the ISE-based data in b, determined by readout uncertainties, are not shown because they are significantly larger than the mean values.

Information, Fig. S2).

We also quantify [Na^+] in the breast milk samples using a G-ISFET Na^+ sensor, bypassing the μED process. The results (Fig. 6a) show a significant discrepancy from the benchmark concentrations determined by ICP-MS, with the maximum concentration difference reaching 2.73 mM, a value comparable to the sodium concentrations themselves. Fig. 6c shows the percentage deviation between [Na^+] measurements obtained from the G-ISFET Na^+ sensor, whether processed by μED or unprocessed, and those determined by ICP-MS: For the measurements involving μED, the deviations are below 9.3 %; for those without μED involvement, they exceed −46.4 %. The concentrations determined without the use of μED are consistently lower than the benchmark concentrations, indicating that the sensitivity of the G-ISFET Na^+ sensor degrades due to biofouling from the complex breast-milk samples when μED is not implemented. Therefore, the use of the μED processor is essential; its combination with the G-ISFET Na^+ sensor enables high-precision quantification of sodium ions in breast milk.

4. Conclusions

We develop a microdevice for high-performance total analysis of sodium ions in breast milk. This device utilizes a μED processor to purify complex biological fluids, streamlining the pre-treatment process and reducing its time and cost. By integrating with a G-ISFET sodium sensor, minimal sample volume is required to offer high-precision sodium-ion quantification at high speed. Compared with other traditional detection methods, our system has significant improvements in overall size, analysis time, and cost-effectiveness while still satisfies the accuracy and range requirements essential for breast-milk sodium detection. Our research holds the potential to address challenges associated with breast-milk sodium levels, such as SCM. Furthermore, it provides a platform technology that can be developed to detect other analytes, such as critical nutrients and heavy-metal ions, in complex biological fluids, paving the way to holistic home health monitoring systems for personalized healthcare.

CRediT authorship contribution statement

Alan T. Charlie Johnson: Writing – review & editing, Resources. **Jianghong Liu:** Writing – review & editing, Resources. **Sallie S. Schneider:** Writing – review & editing, Funding acquisition. **Katie T. Kivlighan:** Writing – review & editing. **Xin Zhang:** Writing – review & editing, Investigation. **Xiaoyu Zhang:** Writing – review & editing, Investigation. **Xiao Fan:** Writing – review & editing, Investigation, Formal analysis. **Huilu Bao:** Writing – original draft, Investigation, Formal analysis, Conceptualization. **Jinglei Ping:** Writing – review & editing, Supervision, Funding acquisition, Formal analysis, Conceptualization. **Kathleen F. Arcaro:** Writing – review & editing, Resources, Formal analysis, Conceptualization.

Declaration of Competing Interest

The authors declare that they have no known competing financial interests or personal relationships that could have appeared to influence the work reported in this paper.

Data availability

All study data are included in the article.

Acknowledgment

J. P., A. T. C. J., and J. L. acknowledge support from Department of Defense (DoD), Congressionally Directed Medical Research Programs (CDMRP) (W81XWH-19–1–0006). K. F. A. and S. S. S. thank support from the National Institutes of Health (NIH) under award number (R01HD111200). Mass spectral data are obtained at the University of Massachusetts Mass Spectrometry Core Facility, RRID: SCR_019063.

Supporting Information

Detailed method section and two figures for resopnse to standard NaCl solutions (additional data), along with Bland-Altman plots.

Appendix A. Supporting information

Supplementary data associated with this article can be found in the online version at doi:10.1016/j.snb.2024.136652.

References

[1] C.D.C. Facts About Nationwide Breastfeeding Goals. *Centers for Disease Control and Prevention* ⟨https://www.cdc.gov/breastfeeding/data/facts.html⟩ (2023).
[2] Exclusive breastfeeding for optimal growth, development and health of infants. ⟨https://www.who.int/tools/elena/interventions/exclusive-breastfeeding⟩.
[3] E.C. Odom, et al., Reasons for earlier than desired cessation of breastfeeding, Pediatrics 131 (2013) e726–e732.
[4] H.M. Wren-Atilola, et al., Infant growth faltering linked to subclinical mastitis, maternal faecal–oral contamination, and breastfeeding, Matern. Child. Nutr. 15 (2019) e12756.
[5] T.M. Samuel, et al., Subclinical mastitis in a european multicenter cohort: prevalence, impact on human milk (HM) composition, and association with infant HM intake and growth, Nutrients 12 (2020) 105.
[6] A. Esquerra-Zwiers, et al., Use of a portable point-of-care instrumentation to measure human milk sodium and potassium concentrations, Breastfeed. Med. 17 (2022) 46–51.
[7] M.L. Astolfi, et al., Optimization and validation of a fast digestion method for the determination of major and trace elements in breast milk by ICP-MS, Anal. Chim. Acta 1040 (2018) 49–62.
[8] ISO 21424:2018(en), Milk, milk products, infant formula and adult nutritionals — Determination of minerals and trace elements — Inductively coupled plasma mass spectrometry (ICP-MS) method. ⟨https://www.iso.org/obp/ui/en/#iso:std:iso:21424:ed-1:v1:en⟩.
[9] T. Van Acker, et al., Inductively coupled plasma mass spectrometry, Nat. Rev. Methods Prim. 3 (2023) 1–18.
[10] E. Bakker, Enhancing ion-selective polymeric membrane electrodes by instrumental control, TrAC Trends Anal. Chem. 53 (2014) 98–105.
[11] M.I. Choudhury, et al., Kidney epithelial cells are active mechano-biological fluid pumps, Nat. Commun. 13 (2022) 2317.
[12] K.M. Hoque, et al., The ABCG2 Q141K hyperuricemia and gout associated variant illuminates the physiology of human urate excretion, Nat. Commun. 11 (2020) 2767.
[13] J. Hu, et al., Rational design of all-solid-state ion-selective electrodes and reference electrodes, TrAC Trends Anal. Chem. 76 (2016) 102–114.
[14] S.-I. Ohira, et al., Electrodialytic ion isolation for matrix removal, Anal. Chem. 84 (2012) 5421–5426.
[15] Y. Sugo, et al., Electrodialytic handling of radioactive metal ions for preparation of tracer reagents, Anal. Chem. 92 (2020) 14953–14958.
[16] S.-I. Ohira, et al., Electrodialytic matrix isolation for metal cations, Talanta 132 (2015) 228–233.
[17] S.Y. Kim, D.Y. Yi, Components of human breast milk: From macronutrient to microbiome and microRNA, Clin. Exp. Pediatr. 63 (2020) 301–309.
[18] C.J. Pedersen, Cycl. polyethers their Complex. Met. salts. *J. Am. Chem. Soc.* 89 (1967) 2495–2496.
[19] T. Huang, et al., Graphene-based ion-selective field-effect transistor for sodium sensing, Nanomaterials 12 (2022) 2620.
[20] I. Fakih, et al., Selective ion sensing with high resolution large area graphene field effect transistor arrays, Nat. Commun. 11 (2020) 3226.
[21] M. Xue, et al., Integrated biosensor platform based on graphene transistor arrays for real-time high-accuracy ion sensing, Nat. Commun. 13 (2022) 5064.
[22] I. Fakih, et al., High resolution potassium sensing with large-area graphene field-effect transistors, Sens. Actuators B Chem. 291 (2019) 89–95.
[23] S. Zhang, et al., Efficient removal of metal ions from the ionic liquid aqueous solution by selective electrodialysis, Sep. Purif. Technol. 295 (2022) 121322.
[24] H. Zhou, et al., Separation of hydrochloric acid and oxalic acid from rare earth oxalic acid precipitation mother liquor by electrodialysis, Membranes 13 (2023) 162.
[25] J. Ping, et al., Scalable production of high-sensitivity, label-free DNA biosensors based on back-gated graphene field effect transistors, ACS Nano 10 (2016) 8700–8704.
[26] C. Mackin, et al., A current–voltage model for graphene electrolyte-gated field-effect transistors, Electron Devices IEEE Trans. 61 (2014) 3971–3977.
[27] K. Maksymiuk, et al., Unintended changes of ion-selective membranes composition—origin and effect on analytical performance, Membranes 10 (2020) 266.
[28] B. Fenech-Salerno, et al., A sprayed graphene transistor platform for rapid and low-cost chemical sensing, Nanoscale 15 (2023) 3243–3254.

[29] L. Wang, et al., One-dimensional electrical contact to a two-dimensional material, Science 342 (2013) 614–617.
[30] K.S. Novoselov, et al., A roadmap for graphene, Nature 490 (2012) 192–200.
[31] H. Li, et al., Graphene field effect transistors for highly sensitive and selective detection of K^+ ions, Sens. Actuators B Chem. 253 (2017) 759–765.
[32] Inorganic Applications Team & PerkinElmer, Inc. Analysis of Milk for Major and Trace Elements by ICP-MS. ⟨https://resources.perkinelmer.com/lab-solutions/resources/docs/app_013376_01_nexion_2000_icp-ms_milk_app_note.pdf⟩.
[33] EasyLyte. Medica Corporation ⟨https://www.medicacorp.com/products/electrolyte-analyzers/easylyte/⟩ (2013).
[34] Wilbur, Steve. A comparison of the relative cost and productivity of traditional metals analysis techniques versus ICP-MS in High Throughput commercial laboratories. (2005).
[35] Medica EasyLyte Na K. | 2001 | EasyLyte Electrolyte Analyzers. *Lab Advanced Solutions (LAS)* ⟨http://www.blockscientific.com/shop/product/2001-medica-easylyte-na-k-analyzer-5500⟩.
[36] Mass Spectrometry: Core Facilities. ⟨https://www.umass.edu/ials/mass-spectrometry⟩.
[37] Solutions Pack, 2122, Medica EasyLyte Solutions Pack, NA/K/Li 800mL. *Lab Advanced Solutions (LAS)* ⟨http://www.blockscientific.com/shop/product/2122-medica-easylyte-solutions-pack-na-k-li-800ml-5557⟩.

Huilu Bao is pursuing a Ph.D. in Mechanical Engineering at the University of Massachusetts Amherst. He earned his B.E. and M.E. degrees from Zhejiang Normal University. His research interests include biosensors and developing devices for point-of-care diagnostics.

Xiao Fan is pursuing a Ph.D. in Mechanical Engineering at the University of Massachusetts Amherst. He earned his B.E. degree from Beijing University of Chemical Technology. His research focuses on developing graphene-based nanomaterials for biosensing and biocontrol.

Xiaoyu Zhang is pursuing a Ph.D. in Mechanical Engineering at the University of Massachusetts Amherst. His research interests include understanding transduction properties at nano-bio interfaces and their applications in healthcare and diagnostics.

Xin Zhang is pursuing a Ph.D. in Mechanical Engineering at the University of Massachusetts Amherst. She earned her B.E. and M.E. degrees from Taiyuan University of Technology. Her research interests include studying various cellular phenomena under different microenvironmental stimulations.